Journal of Ultrafine Grained and Nanostructured Materials
https://jufgnsm.ut.ac.ir
Vol. 56, No.2, December 2023, pp. 224-232
Print ISSN: 2423-6845 Online ISSN: 2423-6837
DOI: 10.22059/jufgnsm.2023.02.11

The effect of SPION size and salting-out on transduction of PEGylated lentiviral vector

Hamed Omid[1,2,3], Amirhosein Paryab[2], Yasamin Nakhli[2], Nasim Sajadi[4], Hamid Reza Madaah Hosseini[2,*], Naser Ahmadbeigi[1,3,*], Alexander M. Seifalian[5]

[1]Gene Therapy Research Center, Digestive Disease Research Institute, Tehran University of Medical Sciences, Tehran, Iran;

[2]Department of Materials Science and Engineering, Sharif University of Technology, Azadi Avenue, Tehran, Iran;
[3]SABZ Biomedicals Science-Based Company, Tehran, Iran;
[4]Ali-Asghar Children Hospital, Iran University of Medical Sciences, Tehran, Iran;
[5]Nanotechnology & Regenerative Medicine Commercialisation Centre (NanoRegMed Ltd, Nanoloom Ltd, & Liberum Health Ltd), London BioScience Innovation Centre, London, UK.

Recieved: 1 December 2023; Accepted: 27 December 2023

**Corresponding author email: n-ahmadbeigi@tums.ac.ir, madaah@sharif.edu*

ABSTRACT

Gene editing has many promising applications for the treatment of diseases with unmet clinical needs, including cancers and autoimmune. There are two main routes for gene delivery: viral and non-viral. Recent research shows viral methods are emerging in clinical trials. Nevertheless, there are still a couple of technological obstacles that require further improvements, these include virus concentration and low efficiency of transduction. This research aimed to employ superparamagnetic iron oxide nanoparticles (SPION) to solve these problems. Three sizes of 10, 40, and 120 nm SPION were synthesized by co-precipitation and Sol-Gel methods, and characterized by XRD, FTIR, FESEM, and VSM. Conjugating SPION to viruses by polyethylene glycol (PEG) can increase the sedimentation of viruses due to magnetic and gravity forces even without ultracentrifuge. Moreover, this magnetic force can guide viruses toward cells and tremendously facilitate the transduction process. As shown, average size SPION (40 nm) revealed the best performance, especially in combination with salting-out precipitation and increased transduction efficiency of more than 20-fold. SPION size has significant effects and should be considered for this application. The combination of the salting-out method and SPION has a synergic effect and elevates transduction results tremendously.

Keywords: *SPION; Nanoparticles; Transduction; Gene editing; lentivirus; PEG.*

1. Introduction

Genetics is one of the fast-growing fields with diverse promising visions including gene therapy. The gene inserting or eliminating that is known as gene-editing technology gives us the treatment ability of genetic disorders or maybe in the future the improvement of genomes. Many diseases do not respond to molecular therapy, and in turn, need cellular therapy with trained cells. The CAR-T cells developed independently by several research groups in the 1980s is an example of it [1, 2].

There had been innumerable research in this field but getting the first FDA approval for gene-edited cells (KYMRIAH™, tisagenlecleucel) was a turning point. The initial use of gene-editing in people was in 2014 when the clinical trials of gene-edited cells were employed to treat HIV patients [3]. The zinc-finger nuclease (ZFN) enzyme

was used in an ex vivo setup to cut out the gene responsible for the T cells' protein targeted by HIV. Then gene-edited T cells were injected into the patients. This method revealed a promising opportunity for HIV treatment. Interestingly, in vivo gene editing also becomes possible. Sharma et al. in 2015 employed ZFN-mediated site-specific integration of transgenes by an adeno-associated viral (AAV) vector for long-term expression of human factors VIII ND IX in mouse models of hemophilia A and B [4].

There are several severe and prevalent diseases including cancers, autoimmune, and inherited diseases which can be cured by gene editing. Among transduction methods, viral vectors are much closer to clinical trials. However, some barriers cause low efficiency and slow kinetics for both transfection and transduction. One of these barriers is the low concentration of DNA at the cell surface [5] due to the high colloidal stability of viruses in biological media and the repulsive electric force on the cell membrane (both have a negative charge). To solve the problem, a range of solutions has been suggested including cationic ions, polymers, liposomes, needle injection, biolistic gun, electroporation, microfluidic, etc [6-12].

These methods were employed to deposit vectors on the cell surface. Researchers have used simple techniques such as removing media before transduction, giving several incubation hours, or raising MOI (Multiplicity of Infection) to increase viral vectors contact with cells, however, these techniques were not applicable to clinical applications. Removing media and incubation time are irrelevant to in vivo, and increasing MOI has tumor genesis issues. Moreover, one of the requirements of clinical application is the large-scale production of viruses which is costly. Hence, it's important to find a suitable methodology clinically applicable to increase the efficiency of transduction inexpensively without serious side effects.

SPION is well-known in medical and biological applications [13-17]. For the transfection process, SPION has been used which became well-known as the "magnetofection" method with positive outcomes [18]. In this work, we employed SPIONs for the transduction process which had several advantages. First, the highly weighted metal oxide particles facilitated the viral concentration and eliminated the ultracentrifuge necessity. Second, magnetic forces could increase transduction efficiency and decrease its time immensely. Third, iron oxide NPs are FDA-approved and trackable in transduced cells by Magnetic resonance imaging (MRI) [17]. This work showed that "magnetoduction", using magnetic NPs for transduction, is as fruitful as magnetofection.

2. Materials and Methods

2.1. Materials

Iron (III) chloride hexahydrate ($FeCl_3.6H_2O$), Iron(II) chloride tetrahydrate ($FeCl_2.4H_2O$), sodium hydroxide (NaOH), potassium nitrate (KNO_3), Iron (II) sulfate heptahydrate ($FeSO_4.7H_2O$), potassium hydroxide (KOH), and polyethylene glycol -6000 (PEG) were all purchased from Merck and used without further treatment. 3-[4,5-dimethylthiazol-2-yl]-2,5-diphenyl tetrazolium bromide (MTT) was purchased from Sigma-Aldrich.

2.2. Synthesis and PEG functionalization of magnetite nanoparticles

2.2.1. Co-precipitation synthesis of magnetite nanoparticles

Co-precipitation synthesis was done in order to provide 2 samples. Their processes are different in terms of reactant concentrations and base addition rate which leads to 2 samples namely NP1 and NP2 (Table 1). All steps were carried out at room temperature. First, 0.002 mol of $FeCl_3.6H_2O$ and 0.001 mol of $FeCl_2.4H_2O$ were dissolved in 10 mL (NP1) and 50 mL (NP2) DI water in two different beakers. Then, 0.008 mol of NaOH was dissolved in 10 mL (NP1) and 50 mL (NP2), separately. For the NP1 sample, the iron chloride solution was added to the base solution at the rate of 1mL/min and for the NP2 sample, 5 mL of the base solution was added into the iron chloride solution every five minutes

Table 1- Physicochemical properties of the SPIONs

Samples	Preparation Method	size (nm)	Magnetization (emu/g)
NP1	Co-precipitation	10	35.83
NP2	Co-precipitation	40	56.11
NP3	Sol-Gel	120	45.36

until it was finished. Both samples were magnetically decantated and washed once with ethanol and twice with DI water. The nanoparticles were dispersed in DI water and kept for subsequent treatment [19].

2.2.2. Sol-Gel synthesis on magnetite nanoparticles

This method was carried out according to the paper published by Sugimoto in 1979 [20]. First, DI water was bubbled by N_2 gas in order for O_2 in water to be eliminated. Then, 2 mL of 1.25 M KOH solution and 2 mL of 2 M KNO_3 solution were prepared and added into a 50 mL volume three neck reactor. The reactor was heated to 50 ˚C in an oil bath. After 15 minutes, 6 mL of 0.0416 M $FeSO_4.7H_2O$ solution was added to the reactor. At this moment a green precipitate was formed inside the reactor. The temperature was raised to 90 ˚C and the system was aged for 4 hours. The whole process was carried out in N_2 gas purge. After synthesis, the nanoparticles were dispersed with ultrasound and centrifuged so that the unreacted ions could be freed from intraparticle voids (NP3). This treatment was done three times and the nanoparticles were kept in water for subsequent treatments.

2.2.3. PEG functionalization of nanoparticles

Synthesized nanoparticles were first dried at 60 ˚C for 72 hours. Then, 0.2 g of nanoparticles was taken and put into a beaker. Following that, 0.2 g of PEG and 30 mL of DI water were added into the same beaker and transferred to the ultrasound setup. The whole system was subjected to regular pulses for 5 minutes. After that, the nanoparticles were centrifuged and excess PEG was removed from the solution.

2.3. Characterization of SPIONs

X-ray diffraction method was performed for phase analysis using XRD, Panalytical-2009, Cambridge, the U.K employing Cu K_α radiation (0.15418 nm). Scherrer method was employed in Phillips X'Pert Highscore. FT-IR test was carried out to investigate functional groups on the nanoparticles using a Bruker Vertex 70 FT-IR instrument (Bruker, USA). Field Emission Scanning Electron Microscope (FE-SEM, TeScan Mira III, Brno, Czech Republic) was used to study the morphology of the particles. Also, to study the magnetic properties of Fe_3O_4 nanoparticles a vibrating sample magnetometer (VSM) experiment was carried out with an HH15 apparatus between 10-4 and 104 G.

2.4. Cell lines and culture

The Lenti-X 293T cell line was purchased from the Iranian Biological Resource Center, Tehran, Iran. The Cells were cultured in high glucose Dulbecco's Modified Eagle's Medium (DMEM) with 10% fetal bovine serum (FBS) supplement, Streptomycin 100 µg/mL, and Penicillin (All from Gibco) under a humidified air with 5% CO_2 at 37°C.

2.5. Lentiviral vector production

3×10^5 Lenti-X 293T cells were seeded in a T-25 flask and incubated at 37 ˚C, 5% CO_2 for 24 h. 21 µg of three vectors (pCDH : pSPAX2 : pMD2.G = 2 : 2 : 1) were diluted in NaCl 150 mM to reach total volume of 1.5 mL. 10 µL of PEI (40 KD) was diluted in 40 µL of NaCl 150 mM and added 84 µL of PEI solution to the vectors sample. After vortexing, the mixture incubated for 15 minutes at room temperature. The culture medium of the flask was removed and the prepared transfection solution added to it. New culture medium and serum added to flask 30 minutes after transfection. The lentiviral particles were collected from supernatant at 24, 48, and 72 h after transfection. The collected viral soups were pooled, filtered, and stored at -80 ˚C [21].

2.6. Magnetoduction

3×10^4 Lenti-X 293T cells were seeded in a 24-well plate and incubated for 24 h. The mixture of NPs (0.5mg Fe) and 200 µL PEG 50 % after thorough sonication added to 1.5 mL of prepared viral soup in a 2 mL Eppendorf tube, then 50 µL NaCl 5 M added to the tube and shook for 6 h in 4 ˚C. Afterward, the tube centrifuged for 20 min at 4000 g, 4˚ C. For salting-out samples before centrifuge 100 µL NaCl 5 M was added. The supernatant was removed and the remnant was added to the cells without culture medium. After transducing cells for 2 h, fresh medium added to wells and incubated for 3 days, then cells were ready for flow cytometry.

2.7. Flow cytometry

After transduction, the GFP (green fluorescent protein) percent of trypsinized cells can be measured by flow cytometry, Facscalibur, BD Biosciences-US. For accurate statistical calculation, the GFP percent should be lower than 30%. A lower GFP percentage eliminates the probability of multi-entrance of particles to a single cell. By decreasing viral soup volume, we can decline the GFP

percent. According to equation (1), the number of viral particles per 1μL can be achieved statistically.

$$\text{Particle per } \mu L = \frac{\text{number of cells} * \text{GFP\%}}{\text{Viral soup vol } (\mu L)} \quad (1)$$

2.8. Cell Viability Assay

The viability of lenti-X 293 cells was assayed using MTT assay. Cells were incubated with viral soup, viral soup-PEG, and viral soup-PEG-NPs in a 96-well plate. Concentrations in the MTT assay were the same as the ones used in the transduction process. After 24h incubation at 37°C, mediums were replaced by 0.5mg/mL MTT solution. In the transduction process, cells were exposed for 2h to this concentration, but for the MTT assay exposure time was extended to 24h to exaggerate cytotoxicity.

3. Results

3.1. Characterization of synthesized NPs

Figure 1 (A) shows the XRD patterns of the synthesized nanoparticles. The pattern is well-matched with the magnetite (Fe_3O_4) diffraction peaks (JCPDS card no. 19-0629) and confirms the inverse spinel structure in all samples. Obviously, by decreasing NPs size the intensity of peaks reduces [22]. Low intensity and wider peaks increase full wide at half maximum (FWHM) which has a reciprocal relation with crystalline size according to the Scherrer equation. These size results were in accordance with FE-SEM data.

FTIR spectra of PEG-6000 and unmodified nanoparticles are shown in figure 1 (B). The stretch and the vibration band of ether -C-O-C- are visible in the PEG spectrum at 1101 cm^{-1} and 1349.4 cm^{-1}, respectively [23]. The 1464 cm^{-1} transmittance band attributes to the vibration of $-CH_2$ [24] and the peak near 950 cm^{-1} corresponds to the out-of-plane bending vibration of -CH. The transmittance band at 578 cm^{-1} represents the stretching mode of Fe-O in Fe_3O_4 [25]. The wide peak of 3450 cm^{-1} in both spectra represents the attached hydroxyl groups [23]. In the SPION-PEG spectrum, the transmittance of ether stretch and $-CH_2$ vibrational bands can confirm the existence of PEG on the particles' surface. This spectrum had a negligible shift

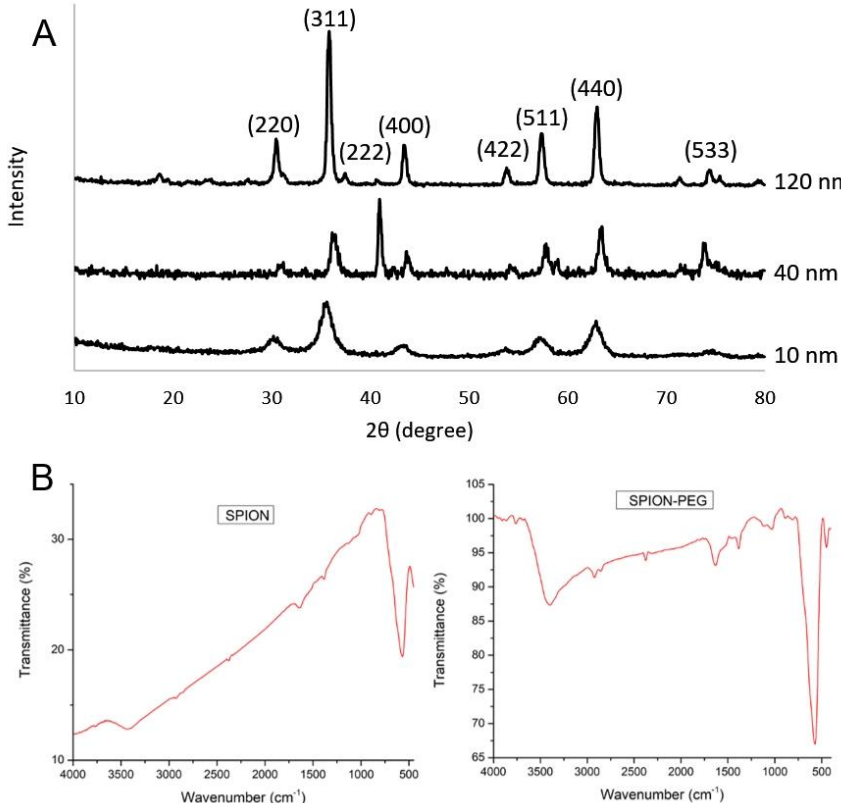

Fig. 1- XRD pattern of synthesized 10, 40 and 120 nm iron oxide particles (A), and FTIR spectrum of SPION and SPION-PEG (B).

rather than free PEG. Due to attaching the polymer to the surface of the particles, it shows lower frequencies [23].

FESEM micrograph and size dispersity of the synthesized samples were shown in figure 2. According to FESEM images, NPs' core sizes were measured and NP percentage in each interval was plotted. As presented 10, 40 and 120 nm are mode sizes in samples NP1, NP2, and NP3, respectively. Smaller NPs in the same concentration have a larger surface-to-volume ratio which increases surface energy and colloidal stability. Higher surface energy intensifies bounding tendency, and more stability increases the number of colloidal collisions between NPs and viruses. Both of these parameters enhance virus fishing from the viral soup and improve the efficacy of viral concentrating without ultracentrifuge. However, higher surface energy increases the agglomeration of NPs and declines to catch viruses. Smaller NPs have lower weight and lower gravity force to sediment viruses. Accordingly, the small size of NPs has advantages and disadvantages in this application, and this article revealed there is an optimum size for it.

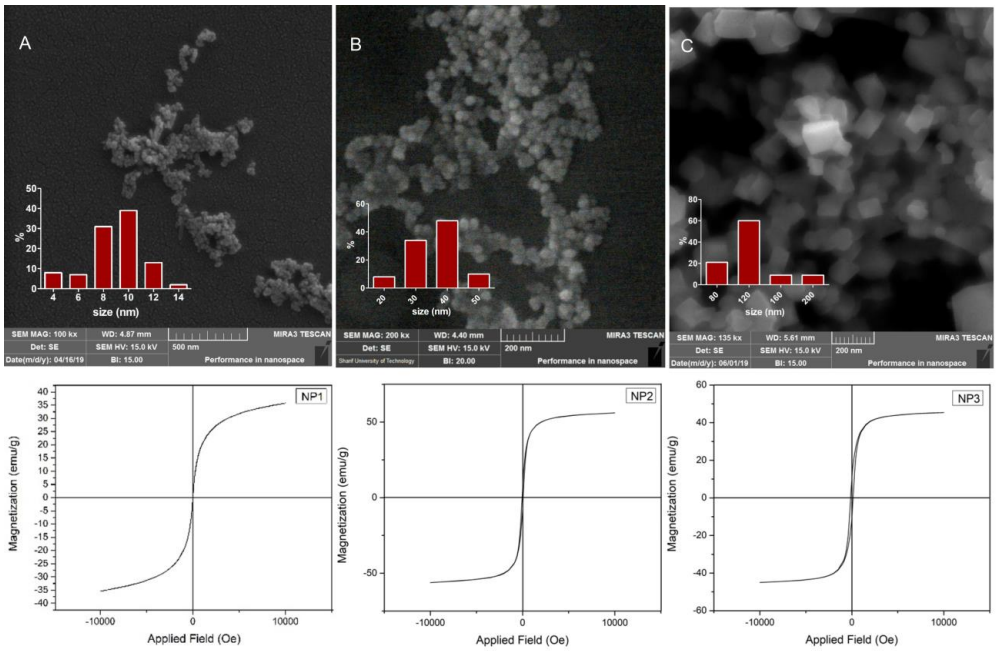

Fig. 2- FESEM micrographs with size dispersity plots for NP1, NP2 and NP3 samples with 10, 40 and 120 nm mode sizes, respectively. VSM results of each synthesized NPs shows their magnetic properties, the NP2 with 50 emu/g the highest saturation.

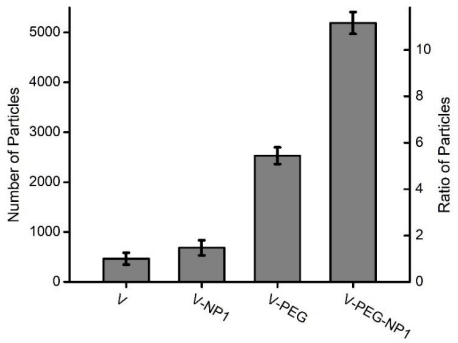

Fig. 3- Binding ability of NPs to the lentivirus by counting number of viral particles that successfully entered Lenti-X 293T cell line in transduction process. V, V-NP1, V-PEG and V-PEG-NP1 are mere viral soup, mixture of viral soup and NP1 sample, mixture of viral soup and PEG, and mixture of viral soup, PEG and NP1, respectively.

Figure 2 represents hysteresis loops of iron oxide NPs by VSM. Sample NP1 shows perfect superparamagnetism and by increasing the size of NPs superparamagnetic behavior disappears. However, coercivity is still negligible in NP2 and NP3. Sample NP2 has the highest magnetization. In very large particles, the hysteresis loop area increases which means these particles can save magnetism. This remaining magnetism causes higher attraction force and more agglomeration. Hence, NP2 seems to have optimum magnetic behavior, higher magnetization, and lower coercivity which concluded to higher response to the magnetic field and higher colloidal stability.

3.2. Binding ability of NP to the lentivirus

Due to the high surface energy of NPs, some of them bind to the viruses and increase transduction efficacy by about %50. In figure 3, V is the viral soup sample, V-NP1 is a mixture of viral soup with NP1 sample, and V-NP1 is 1.5 fold of V. However, PEG has a much better binding ability to viruses and shows near 6-fold improvement rather than the V sample. Hence, PEG was used to increase the binding between NPs and viruses and revealed a synergic effect more than 11-fold (V-PEG-NP1).

3.3. Evaluating transduction efficiency with GFP expression

Figure 4 reveals flow cytometry results for the transduction process by three different NP sizes and salting-out method in similar condition. Figure 4 (A) shows the GFP expression of transduced cells by 50μL centrifuged viral soup. Figure 4 (B, D, F) represents the results of transduction by 3μL centrifuged virus, PEG, and NP complex, and figure 4 (C, E, G) shows the salting-out method of these three complexes. Obviously, NP2 (figure 4 D and E) shows higher GFP expression, and the NP3 complex (figure 4 F and G) was the worse one. The salting-out method had a good synergic on NP1 and NP2 by accelerating sedimentation of virus-PEG-NP complex but made NP3 sample worse.

3.4. Targeted gene delivery

Magnetic NPs in addition to efficacy enhancement of the transduction are able to deliver the vector to a specific area. This control would be worthwhile particularly in in-vivo gene delivery. As shown in figure 5, in areas with most NPs accumulation there is more GFP expression. Due to the attachment of viruses to NPs, areas with NPs aggregate are enriched virus ones and have a higher probability of transduced cells.

3.5. Effect of SPIONs' size

Comparison of magnetoduction with three different sizes of NPs revealed that size has undeniable roles on the efficiency of transduction. White columns in figure 6 represent NP2 with 40 nm average size has the highest efficiency, around 1100 %. NP1 with the best stability but lowest weight and magnetic force has the second position. The largest sample (NP3) due to low colloidal stability has the worst result. The grey columns are the salting-out method and exhibit a synergic effect on NP1 and NP2. Increasing ion strength can destabilize the colloidal system and accelerate sedimentation of the V-PEG-NP complex. By contrast, its antipathy on NP3 is obvious. NP3 is the unstable one and salting-out makes it worth, and rapid sedimentation of NPs prevents collision and attachment between viruses and NPs. It can be concluded the combination of NP with average size and salting-out method is the best option for magnetoduction that increases the efficiency more than 20-fold.

3.6. Cytotoxicity of magnetoduction

MTT assay (figure 7) revealed that neither lentivirus, PEG nor NPs have significant cytotoxicity on the Lenti-X293T cells after 24 h. However, the NP2 and NP3 samples declined the cell proliferation to about 90 % and 80 %, respectively. In the transduction process, a new culture medium can be added after 2 h that eliminates most of the NPs, and just NPs that entered cells remain. Hence, the toxicity of a high load of NPs doesn't cause serious concern.

4. Discussion

Nanosize viruses have good stability in media and it is difficult to concentrate them without employing ultracentrifuge. In very high G-force, the exerted shear stress on viruses increases tremendously which can damage them. There is a large number of researches on eliminating ultracentrifuge necessity [26, 27].

Wei Jiang et al. [28] revealed that due to the fragile nature of lentivirus not only high G-force but also acceleration or brake speed can damage them significantly. However, using heavy metallic NPs and magnetic force can accelerate the sedimentation of viruses without any mechanical harm. Moreover, putting out samples from ultracentrifuge and carrying them have enough shaking to

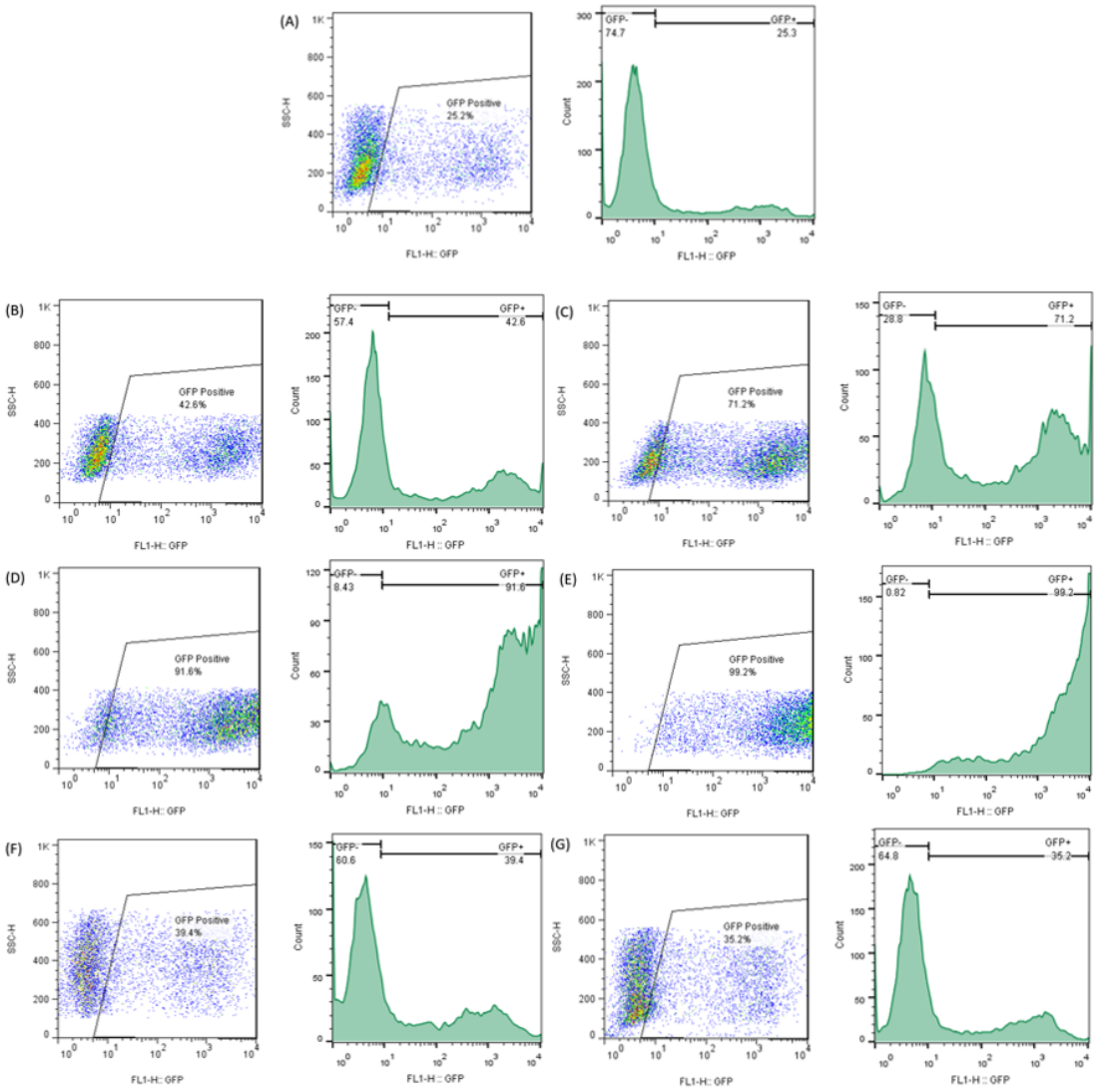

Fig. 4- Assessment of GFP expression in Lenti-X293T cells by flow cytometry. Transduction was done by mere viral soup (A), NP1 (B), NP1+S (C), NP2 (D), NP2+S (E), NP3 (F), NP3+S (G). For B-G, complexes of 3µL viral soup, PEG, and NP was used. E, F and G are salting out (+S) of B, C and D, respectively.

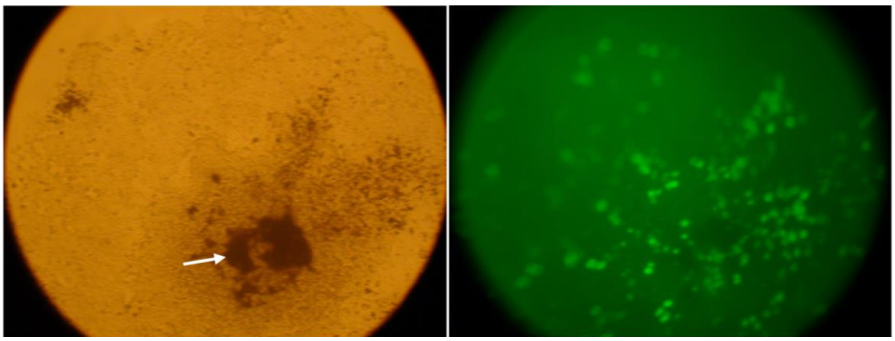

Fig. 5- Optical microscopic image of Lenti-X 293T cells after transduction (Left), the dark spots are iron oxide NPs agglomeration. GFP expression in Lenti-X 293T 72h after magnetoduction under fluorescence microscopy (Right) (20× magnification).

lose some portion of them that would be costly in the large-scale application. But attaching the virus to magnetic NP gives us the ability to concentrate them anytime, and the polymeric net of PEG minimizes the virus loss. Being time-effective and inexpensive makes this method suitable for clinical trials.

NP1 has a small size and high stability, therefore it can catch viruses better, and using the salting-out method for these particles shows huge improvement. On the other hand, NP3 has the largest size and lowest stability. Hence, the salting-out method makes its stability worse and decreases virus fishing. Finally, the NP2 sample with average size revealed the best performance. It has both stability and weight to fish viruses and concentrates them.

5.Conclusion

Our results indicated that the size of SPIONs has a vital role in the efficiency of magnetoduction. For transduction of HEK 293T cells by lentivirus, iron oxide NP with an average size of 40 nm had a greater outcome, and combining it with the salting-out method showed a synergistic effect. These NPs are FDA approved for other applications and suitable for clinical trials. On the other hand, they are inexpensive in comparison to other methods which makes them appropriate for large-scale applications. The magnetic force of these NPs precipitates viruses in cells and improves the efficiency of transduction even in low MOIs. Low MOI decreases virus consumption, lowers expenses of therapy, and reduces tumor genesis side effects of high gene loads.

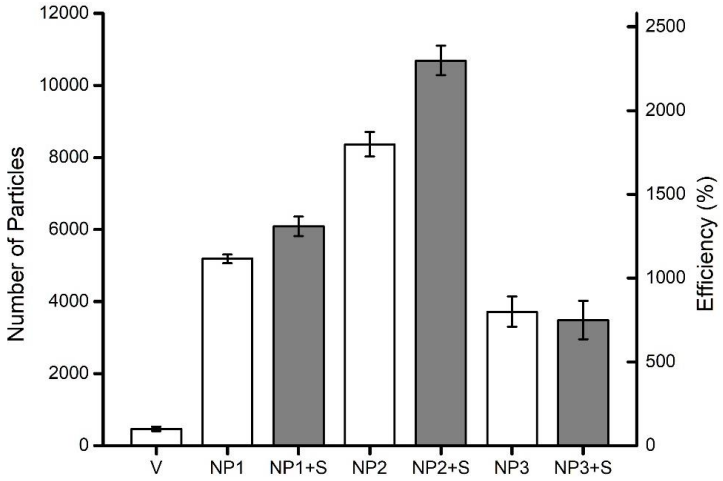

Fig. 6- XRD pattern of synthesized 10, 40 and 120 nm iron oxide particles (A), and FTIR spectrum of SPION and SPION-PEG (B).

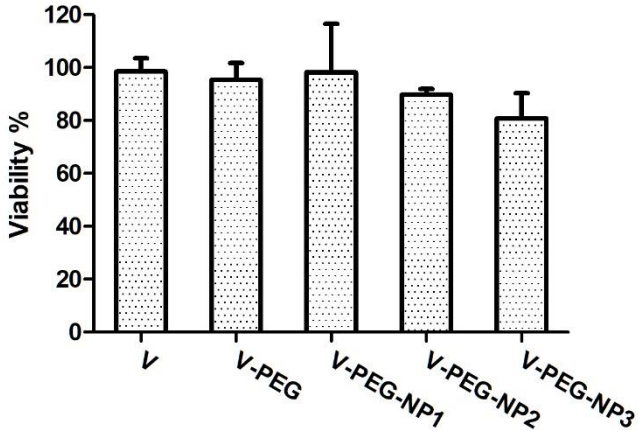

Fig. 7- Viability of Lenti-X 293T cell line treated with viral soup (V), viral soup and PEG (V-PEG), and finally viral soup, PEG and NP samples (V-PEG-NP1 to 3) at 24h.

References

1. Kuwana Y, Asakura Y, Utsunomiya N, Nakanishi M, Arata Y, Itoh S, et al. Expression of chimeric receptor composed of immunoglobulin-derived V resions and T-cell receptor-derived C regions. Biochemical and Biophysical Research Communications. 1987;149(3):960-8.
2. June CH, Ledbetter JA, Gillespie MM, Lindsten T, Thompson CB. T-Cell Proliferation Involving the CD28 Pathway Is Associated witH Cyclosporine-Resistant Interleukin 2 Gene Expression. Molecular and Cellular Biology. 1987;7(12):4472-81.
3. Tebas P, Stein D, Tang WW, Frank I, Wang SQ, Lee G, et al. Gene editing of CCR5 in autologous CD4 T cells of persons infected with HIV. N Engl J Med. 2014;370(10):901-10.
4. Sharma R, Anguela XM, Doyon Y, Wechsler T, DeKelver RC, Sproul S, et al. In vivo genome editing of the albumin locus as a platform for protein replacement therapy. Blood. 2015;126(15):1777-84.
5. Luo D, Saltzman WM. Enhancement of transfection by physical concentration of DNA at the cell surface. Nature Biotechnology. 2000;18(8):893-5.
6. Bishop NE, Anderson DA. Early interactions of hepatitis A virus with cultured cells: viral elution and the effect of pH and calcium ions. Archives of Virology. 1997;142(11):2161-78.
7. Rivière GN, Korpi A, Sipponen MH, Zou T, Kostiainen MA, Österberg M. Agglomeration of Viruses by Cationic Lignin Particles for Facilitated Water Purification. ACS Sustain Chem Eng. 2020;8(10):4167-77.
8. Saito K, Otsuki N, Takeda M, Hanada K. Liposome Flotation Assay for Studying Interactions Between Rubella Virus Particles and Lipid Membranes. Bio Protoc. 2018;8(16):e2983-e.
9. Cearley CN, Wolfe JH. A single injection of an adeno-associated virus vector into nuclei with divergent connections results in widespread vector distribution in the brain and global correction of a neurogenetic disease. Journal of Neuroscience. 2007 Sep 12;27(37):9928-40.
10. Thomas J-L, Bardou J, L'Hoste S, Mauchamp B, Chavancy G. A helium burst biolistic device adapted to penetrate fragile insect tissues. Journal of Insect Science. 2001;1(9):1-10.
11. Kurita H, Takahashi S, Asada A, Matsuo M, Kishikawa K, Mizuno A, Numano R. Novel Parallelized Electroporation by Electrostatic Manipulation of a Water-in-Oil Droplet as a Microreactor. PLoS One. 2015;10(12):e0144254-e.
12. Lissandrello CA, Santos JA, Hsi P, Welch M, Mott VL, Kim ES, et al. High-throughput continuous-flow microfluidic electroporation of mRNA into primary human T cells for applications in cellular therapy manufacturing. Sci Rep. 2020;10(1):18045-.
13. Mahmoudi M, Sant S, Wang B, Laurent S, Sen T. Superparamagnetic iron oxide nanoparticles (SPIONs): Development, surface modification and applications in chemotherapy. Advanced Drug Delivery Reviews. 2011;63(1-2):24-46.
14. Allard-Vannier E, Hervé-Aubert K, Kaaki K, Blondy T, Shebanova A, Shaitan KV, et al. Folic acid-capped PEGylated magnetic nanoparticles enter cancer cells mostly via clathrin-dependent endocytosis. Biochimica et Biophysica Acta (BBA) - General Subjects. 2017;1861(6):1578-86.
15. Ahmadi R, Hosseini HRM, Masoudi A, Omid H, Namivandi-Zangeneh R, Ahmadi M, et al. Effect of concentration on hydrodynamic size of magnetite-based ferrofluid as a potential MRI contrast agent. Colloids and Surfaces A: Physicochemical and Engineering Aspects. 2013;424:113-7.
16. Alromi DA, Madani SY, Seifalian A. Emerging Application of Magnetic Nanoparticles for Diagnosis and Treatment of Cancer. Polymers (Basel). 2021;13(23):4146.
17. Wong J, Prout J, Seifalian A. Magnetic Nanoparticles: New Perspectives in Drug Delivery. Current Pharmaceutical Design. 2017;23(20).
18. Scherer F, Anton M, Schillinger U, Henke J, Bergemann C, Krüger A, et al. Magnetofection: enhancing and targeting gene delivery by magnetic force in vitro and in vivo. Gene Therapy. 2002;9(2):102-9.
19. Iwasaki T, Mizutani N, Watano S, Yanagida T, Kawai T. Size control of magnetite nanoparticles by organic solvent-free chemical coprecipitation at room temperature. Journal of Experimental Nanoscience. 2010;5(3):251-62.
20. Sugimoto T, Matijević E. Formation of uniform spherical magnetite particles by crystallization from ferrous hydroxide gels. Journal of Colloid and Interface Science. 1980;74(1):227-43.
21. Gheisari Y, Azadmanesh K, Ahmadbeigi N, Nassiri SM, Golestaneh AF, Naderi M, et al. Genetic Modification of Mesenchymal Stem Cells to Overexpress CXCR4 and CXCR7 Does Not Improve the Homing and Therapeutic Potentials of These Cells in Experimental Acute Kidney Injury. Stem Cells and Development. 2012;21(16):2969-80.
22. Cullity BD. Elements of X-ray Diffraction. Addison-Wesley Publishing; 1956.
23. Gupta AK, Wells S. Surface-Modified Superparamagnetic Nanoparticles for Drug Delivery: Preparation, Characterization, and Cytotoxicity Studies. IEEE Transactions on Nanobioscience. 2004;3(1):66-73.
24. Hu L, Hach D, Chaumont D, Brachais CH, Couvercelle JP. One step grafting of monomethoxy poly(ethylene glycol) during synthesis of maghemite nanoparticles in aqueous medium. Colloids and Surfaces A: Physicochemical and Engineering Aspects. 2008;330(1):1-7.
25. Kim M, Jung J, Lee J, Na K, Park S, Hyun J. Amphiphilic comblike polymers enhance the colloidal stability of Fe3O4 nanoparticles. Colloids and Surfaces B: Biointerfaces. 2010;76(1):236-40.
26. Lentivirus Gene Engineering Protocols. Methods in Molecular Biology: Humana Press; 2010.
27. Yamada K, McCarty DM, Madden VJ, Walsh CE. Lentivirus Vector Purification Using Anion Exchange HPLC Leads to Improved Gene Transfer. BioTechniques. 2003;34(5):1074-80.
28. Jiang W, Hua R, Wei M, Li C, Qiu Z, Yang X, Zhang C. An optimized method for high-titer lentivirus preparations without ultracentrifugation. Sci Rep. 2015;5:13875-.